Enhancement of smectic C mesophase stability by using branched alkyl chains in the auxiliary ligands of luminescent Pt(II) and Pd(II) complexes.

Monica Ilis, Marian Micutz, Florea Dumitrascu, Iuliana Pasuk, Yann Molard, Thierry Roisnel, Viorel Cîrcu

Enhancement of smectic C mesophase stability by using branched alkyl chains in the auxiliary ligands of luminescent Pt(II) and Pd(II) complexes

Monica Ilis,[a] Marian Micutz,[a] Florea Dumitrascu,[b] Iuliana Pasuk,[c] Yann Molard,[d] Thierry Roisnel[d] and Viorel Cîrcu*[a]

[a]*Dept. of Inorganic Chemistry, University of Bucharest, 23 Dumbrava Rosie st, sector 2, Bucharest 020464, Romania, e-mail:* viorel_carcu@yahoo.com, viorel.circu@g.unibuc.ro

[b]*Centre for Organic Chemistry "C. D. Nenitzescu", Romanian Academy, Spl. Independentei 202B, Bucharest 060023, Romania*

[c]*National Institute of Materials Physics, P.O. Box MG-7, Magurele, 077125, Romania*

[d]*Sciences Chimiques de Rennes UMR 6226 CNRS Université de Rennes 1, Avenue du Général Leclerc 35042 Rennes Cedex, France*

Abstract: A novel series of Pd(II) and Pt(II) complexes based on cyclometalated imine ligands and N-benzoylthiourea (BTU) derivatives as auxiliary ligands has been prepared and their liquid crystalline properties as well as photophysical properties have been investigated. The crystal structure of one cyclometalated Pt(II) complex with N-(p-F-phenyl)-N'-benzoylthiourea as co-ligand has been solved. The liquid crystalline properties have been investigated by a combination of DSC, POM and variable temperature powder X-ray diffraction. These new metallomesogens display either a monotropic SmC phase or both SmA and SmC phases depending on the number of alkoxy groups attached to the imine ligand, alkyl chain length or the use of branched alkoxy terminal groups. We found that the introduction of branched alkoxy terminal groups lead to lower transition temperatures and stabilisation of the SmC phase in both Pd(II) and Pt(II) complexes. While the Pd(II) complexes display no emission, the Pt(II) complexes show good emission properties in solution, solid state and PMMA film at room temperature and their investigation is reported.

Introduction

Materials with liquid crystalline properties have found various applications ranging from the manufacturing of LCD to different molecular sensors and detectors, optical switches, spatial light modulator, etc.[1] Introduction of metal ions adds unique magnetic, optical and electric properties to the mesophase besides an interesting structural role when compare to purely organic liquid crystals.[2] Light-emitting metallomesogens were intensively studied in the past years.[3] Mesomorphic materials based on cyclometalated Pd(II) and Pt(II) complexes are of great interest due to various choices for tuning the mesogenic properties of such compounds, as well as other physico-chemical properties such are their promising luminescent properties. It is worth to mention here that room-temperature emissive Pd(II) complexes are much rarer compared to their Pt(II) analogues due to the presence of low-lying metal-centered excited states which leads to a strong tendency of nonradiative deactivation.

So far, the different mesomorphic behaviour and, in some cases, the emission properties of Pt(II) metallomesogens have been reported by several groups, [4] including both mono- and dinuclear compounds. The majority of these reported complexes have one cyclometalated ligand derived from the 2-ppy unit and an auxiliary acetylacetonate derivative, and only few are based on imine compounds.

We would like to show that comparable emission properties can be achieved in simpler Pt(II) systems when the mesomorphic properties could be controlled easier by a variety of options to modify the chemical structure around the Pt atom. Moreover, careful design can lead to lower transition temperatures preventing chemical decomposition and stability of the mesophases near room temperature affording the study of emission properties in the liquid crystalline phase. These complexes are based on cyclometalated imine ligands and N-benzoylthiourea (BTU) derivatives as auxiliary ligands. Recently, we have started to investigate the influence of the alkoxy-substituted BTU derivatives on the thermal behaviour of square-planar Pd(II) and Pt(II) cyclometalated complexes as well as their emissive properties.[5] Such BTU derivatives proved to be very good chelating ligands that posses two very strong donor groups (carbonyl and thioamide), giving rise to neutral metal complexes with *S,O*-coordination.[6] We have shown previously that the use of simple *N*-benzoyl thiourea derivatives as co-ligands together with the *ortho*-metalated

imine fragment destabilize the mesogenic behavior of these complexes and monotropic nematic or smectic A phases were observed.[7] By proper design of alkoxy-substituted BTU derivatives it is possible to obtain different types of liquid crystals and several studies dealing with purely organic liquid crystals based on *N*-benzoylthiourea moiety were reported.[8] In this work we present our results concerning the use of branched-alkoxy-substituted BTU derivatives as co-ligands to generate mononuclear Pd(II) and Pt(II) cyclometalated complexes with Schiff bases. It is well known that branching of the terminal alkoxy chains has a significant influence on the mesomorphic behavior of a liquid crystalline material.

Apart from the possibility to introduce chirality in the molecule, the effect of the branch in the terminal chain is to reduce considerably the melting points and thus the liquid crystal phase stability. Moreover, by introduction of branched terminal chains in the molecule, significant changes of both transition temperatures and mesophase type of the material could be seen.[9] Materials displaying the smectic C phase and, in particular the chiral phase SmC*, were widely studied because of the big technological potential in fast-switching displays and other optoelectronic devices. For this reason we were interested to study the potential influence of terminal alkyloxy chain branching on thermal stability of the smectic C phase of these complexes and we could successfully prepared a Pd(II) complex with SmC phase stable up to room temperature.

Also, the photophysical properties of the Pt(II) complexes were investigated.

Results and Discussion

The preparation of mononuclear Pt(II) and Pd(II) complexes along with the numbering scheme is presented in Fig 1. All the new products were characterized by elemental analysis, IR, ^{1}H and ^{13}C NMR spectroscopy while the liquid crystal properties were investigated by a combination of differential scaning calorimetry (DSC), polarizing optical microscopy (POM) and powder X-ray difraction.

The structure of the new cyclometalated mononuclear complexes can be confirmed readily by IR and ^{1}H-NMR spectroscopy when the coordination of the *N*-benzoylthiourea derivatives in the deprotonated form was confirmed by the disappearence of ν_{NH} (~3300 cm^{-1}) and $\nu_{C=O}$ (~1670 cm^{-1}) frequencies (compare to the IR spectra of free ligands)

together with a shift of ν_{C-N} frequency towards lower wavenumbers. This suggests the absence of NH hydrogen located between carbonyl and thiocarbonyl groups of the benzoyl thioureic moiety. This coordination mode is also supported by ^{1}H–NMR spectroscopy. We have started our study with the synthesis of Pd(II) compounds and then extended to Pt(II) as it is well known that the synthesis of the latter compounds proceeds in low yields.

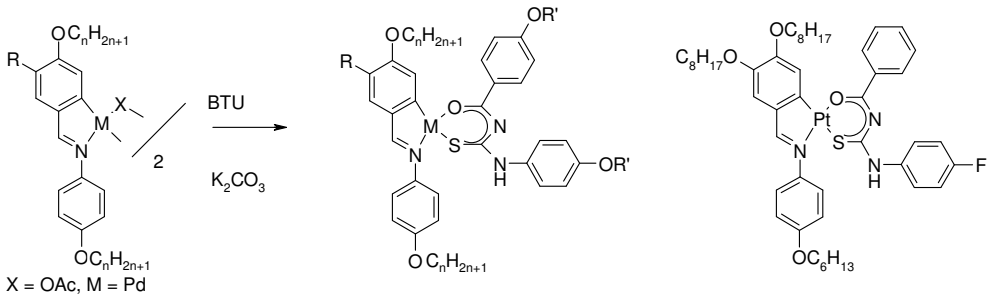

1a, b: M = Pd, R = H, R' = n-octyl, n = 6, 8
1c: M = Pd, R = n-decyloxy, R'= n-octyl, n = 10
2a,b: M = Pd, R = H, R' = 2-ethyl-hexyl, n = 6, 8
2c: M = Pd, R = n-decyloxy, R' = 2-ethyl-hexyl, n = 10
3a,b: M = Pt, R = H, R' = 2-ethyl-hexyl, n = 6, 8
3c: M = Pt, R = n-decyloxy, R' = 2-ethyl-hexyl, n = 10

Scheme 1 Synthetic pathway for Pd(II) and Pt(II) complexes preparation

The intermediate dinuclear chloro-bridged ortho-platinated compounds were obtained by cycloplatination of the Schiff bases using $[Pt(\mu\text{-}Cl)(\eta^3\text{-}C_4H_7)]_2$ as starting material.[4f, 10] These products were used in the next step without further purification. The preparation of mononuclear ortho-platinated complexes **3a-c** and **4** was carried out by ligand exchange reaction of the chloro-bridged dinuclear platinum complexes using the corresponding BTU derivative in the presence of potassium carbonate. The new, mononuclear Pt(II) complexes were obtained in moderate-to-good yields as orange-red, microcrystalline solids. Despite the BTU derivative being unsymmetric, the final products (**3a-c** and **4**) were found to contain only one of the two possible *syn* and *anti* isomers with respect to the positions of sulfur atom of the BTU ligand and nitrogen atom of the metallated Schiff base, most probably the *anti* isomer. This assumption is made on the previously reported results regarding the X-ray crystal structures of related compounds.[7b] Indeed, the isolation of these cyclometalated mononuclear species can be confirmed readily by ^{1}H NMR spectroscopy when a pattern specific to a 1,3,4-substitution of an aromatic ring can be seen as two doublets and a doublet of doublets for complexes having two terminal

alkoxy chains on the imine ligand (**1a,b**, **2a,b** and **3a,b)**. For the remaining complexes, **1c**, **2c, 3c** and **4** two singlets in the aromatic region are seen. All the complexes show the signal corresponding to the imine proton around δ 8 ppm due to a deshielding effect. Additionally, the ^{1}H NMR spectra of Pt(II) complexes show the ^{195}Pt satellites which, once again, confirm the ortho-platination process allowing the coupling constants $^{3}J_{Pt-H}$ to be deduced. The values were in the expected range for such compounds and similar with those found for other ortho-platinated compounds.[11]

Crystal structure description

The attempts to prepare single-crystals of Pt(II) and Pd(II) complexes with branched alkyl-substituted BTU derivatives failed. To confirm the formation of such mononuclear complexes with BTU derivatives as co-ligands we prepared the Pt(II) complex with N-(*p*-F-phenyl)-N'-benzoylthiourea. Indeed, slow crystallization from a mixture of acetone and methanol afforded red crystals that were subjected to X-ray investigation.

The crystallographic data are presented in Table 1 along with selected bond distances and angles in Table 2. The molecular structure of **4** is shown in Figure 1. Complex **4** crystallized in the monoclinic crystal system, space group P21/n, with four discrete molecules in the unit cell. The crystals structure shows the platinum atom surrounded by one sulfur atom and one oxygen atom of the *N*-benzoylthiourea co-ligand, one aromatic carbon atom (metallated phenyl ring) and one nitrogen atom (imine group) belonging to the Schiff base, in an approximately square-planar arrangement with the sulfur atom located *trans* to the nitrogen atom of the imine group.

Table 1 Crystallographic data for complex **4**

Empirical formula	$C_{49}H_{64}FN_3O_4PtS$
Formula weight (g mol^{-1})	1005.18
Temperature (K)	100(2)
Wavelength (Å)	0.71073
Crystal system	Monoclinic
Space group	$P2_1/n$
Unit cell dimensions	
a (Å)	21.4274(5)
b (Å)	8.5266(2)
c (Å)	25.7973(6)
(°)	90
(°)	93.4980(10)
(°)	90
V (Å^3)	4704.46(19)
Z	4
D_{calc} *(Mg m^{-3})*	1.419
μ (mm^{-1})	3.076
F(000)	2056
Colour	Red
Crystal size (mm^3)	0.201 x 0.15 x 0.136
range (°)	2.92 to 27.48
Reflections collected	71938
Independent reflections	10754 [R(int) = 0.0376]
Data / restraints / parameters	10754 / 0 / 536
Goodness-of-fit on F^2	0.978
Final *R* indices [$F^2 > 2(F^2)$]	R1[a] = 0.0193, wR2[b] = 0.0393
R indices (all data)	R1[a] = 0.026, wR2[b] = 0.0417
Largest diff. peak and hole (e·Å^{-3})	0.582 and -0.598

[a] $R1 = \sum | |F_o| - |F_c| | / \sum |F_o|$

[b] $wR2 = \{\sum [w(F_o^2 - F_c^2)^2] / \sum [w(F_o^2)^2]\}^{1/2}$

Table 2 Selected bond distances (Å) and angles (°) for complex **4**

Pt – C	1.9854(19)
Pt – N	2.0453(17)
Pt – O	2.0786(13)
Pt – S	2.2322(5)
N(Ph) – C	1.415(3)
N – C(S)	1.333(2)
N – C(O)	1.339(3)
C – O	1.266(2)
C – S	1.733(2)
C(O) – C(Ph)	1.498(3)
C – N(imine)	1.297(3)
C – Pt – N	80.44(7)
N – Pt – O	92.62(6)
O – Pt – S	93.33(4)
S – Pt – C	93.65(6)

The corresponding chelate ring around Pt centre is essentially planar with the central atom showing no deviation from this mean plane. However, while the metallated phenyl ring is almost coplanar with respect to the mean plane, the unmetallated ring of the imine ligand is twisted by 75.1° with respect to the core plane, as it was previously found for similar orthometallated Pt(II) complexes. We found the Pt-C and Pt-N bond lengths comparable with the values reported for similar *ortho*-platinated complexes with Schiff bases.[12]

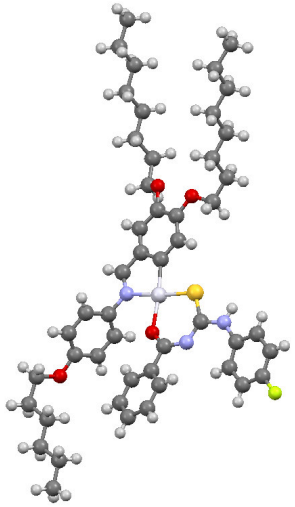

Figure 1. Molecular structure of complex **4**

On the other hand, the Pt–S bond length, 2.232 Å, is comparable with the two values found for the simple *cis* complex of Pt(II) with *N*,*N*-diethyl-*N'*-benzoylthiourea which are 2.231 and 2.233 Å, respectively[13] and similar to that found in cis-bis(*N*,*N*-di(n-butyl)-*N'*-benzoylthioureato)platinum(II), 2.230(2)–2.233(2) Å,[14] but also with the ones found in cyclometalated Pt(II) complexes with 2-phenylpyridine as cyclometalated ligand and *N*,*N*-dipropyl-*N'*-benzoylthiourea and *N*-(p-methoxyphenyl)-*N'*-benzoyl thiourea as auxiliary ligands (2.2389(15) and 2.2447(14) respectively)[15]. We can assume that the relatively long Pt–O bond length (2.079 Å) in complex **4** compare to cis-bis(*N*,*N*-diethyl-*N'*-benzoylthioureato)platinum(II) (2.018 and 2.023 Å)[13] is a consequence of the *trans* influence of the coordinated carbon atom of cyclometallated imine ligand.

The crystal packing of **4** is highly influenced by the contribution of intermolecular –C-H···F-C- interactions, found in the case of fluorine atom of the *N*-benzoylthiourea ligand and the alkoxy group of the metallated ring of imine ligand. The measured H···F distance is 2.44Å which is smaller than the sum of the van der Waals' radii of fluorine and hydrogen at 2.67Å (the van der Waals' radius of fluorine is 1.47Å).[16]

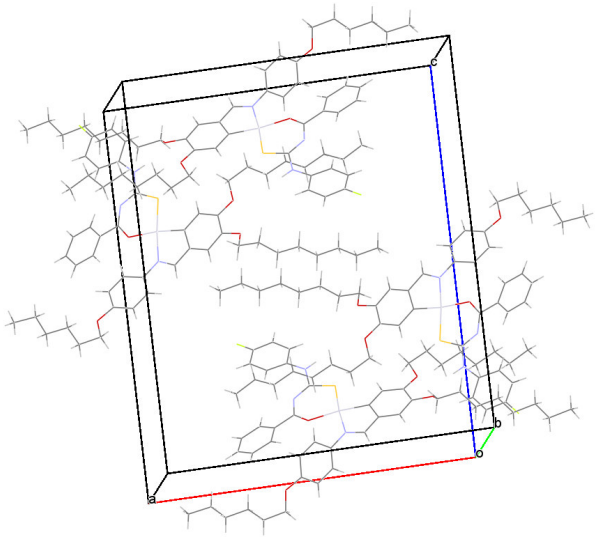

Figure 2. The crystal packing of complex **4**

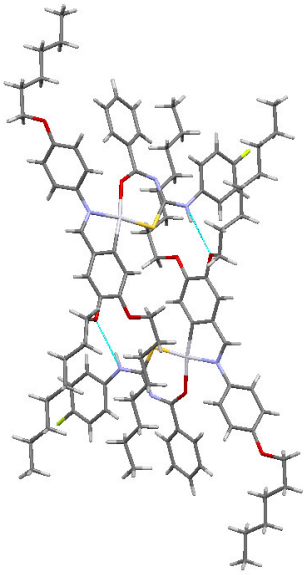

Figure 3. Packing showing the NH…O hydrogen bonds between two adjacent molecules of complex **4**

Short-contacts were also found between the O atom of the alkoxy groups of the metalated ring and the N-H proton of the auxiliary ligand of an adjacent molecule, the measured distance being 2.23 Å. These interactions give rise to 1D - infinite chains connected through NH...O hydrogen bonds. Moreover, the shortest Pt¨Pt distance is 8.527 Å, ruling out any close Pt-Pt interaction in crystalline state and thus, influencing the emission behaviour of **4** in solid-state.

Liquid crystals properties

The liquid crystalline properties of palladium and platinum complexes were investigated by a combination of hot stage polarising optical microscopy (POM), differential scanning calorimetry (DSC) and powder X-ray diffraction. The thermal data are presented in Table 3. The assignment of liquid crystals phases was done based on their optical texture and X-ray measurements.[17] For instance, the SmA phase was assigned based on its characteristic focal fan shape texture with several homeotropic regions when developed from the isotropic state. The SmC phase was assigned based on its broken fan shape texture which was developed either from the isotropic state or from a previously existing SmA phase (Figure 4). The Pd(II) complexes with BTU having unbranched alkyloxy

terminal chains **1a-c** show only one transition on heating corresponding to melting process and two monotropic SmA and SmC phases on cooling from the liquid state. Their melting points slightly depend on the number and length of the chains, with lower transition temperatures for complex **1c** possessing three alkoxy chains on the imine ligand as expected.

Table 3 Phase transition temperatures (^{o}C) and enthalpies ΔH (kJ·mol^{-1}) for Pd(II) and Pt(II) complexes

Complex	Transition	T/°C	ΔH/kJ·mol^{-1}
1a	Cr-I	143	46.1
	(I-SmA)	136	10.8
	(SmA-SmC)	132[a]	
	(SmC-Cr)	114	17.9
1b	Cr-I	137	62.3
	(I-SmA)	136	14.0
	(SmA-SmC)	133[a]	
	SmC-Cr	63	2.7
1c	Cr-Cr'	104	17.0
	Cr'-I	122	24.0
	(I-SmA)	99	16.8
	(SmA-SmC)	97	
	(SmC-Cr)	83	
2a	Cr - I	110	36.3
	(I-SmC)	93	11.6
	(SmC-Cr)	78	15.9
2b	Cr-Cr'	76	4.2
	Cr'-I	96	26.5
	(I-SmC)	90	10.2
	(SmC-Cr)	53	2.5
2c	Cr-Cr'	75	43.4
	Cr'-I	82	11.6
	SmC-SmA	52[b]	1.2
	SmA-I	60[b]	4.2
3a	Cr-I	117	24.7
	(I-SmC)	111	10.9
	(SmC-Cr)	78	5.8
3b	Cr-I	116	29.2
	(I-SmC)	108	10.6
	(SmC-Cr)	82	10.0
3c	Cr-I	103	47.4
	(I-SmA)	73	4.2
	(SmA-SmC)	68	0.8
	(SmC-Cr)	56	8.5
4	Cr – I	112	48.4
	(I – SmA)	(63)	(3.4)

[a]Combined enthalpies, [b]Values taken from the second heating cycle

Three consecutive heating-cooling cycles were recorded for these complexes. The transition temperatures recorded both on heating and cooling the samples are slightly shifted on going from one cycle to the next one. This observation could indicate a partial decomposition of the products. For this reason we undertook a TG study of these products and the decomposition curves are presented in Figure S1 (ESI). These products show an weight loss of approximately 5% around 150°C slightly above the clearing points, and this poorer thermal stability could be responsible for shifting the transition temperatures recorded by DSC.

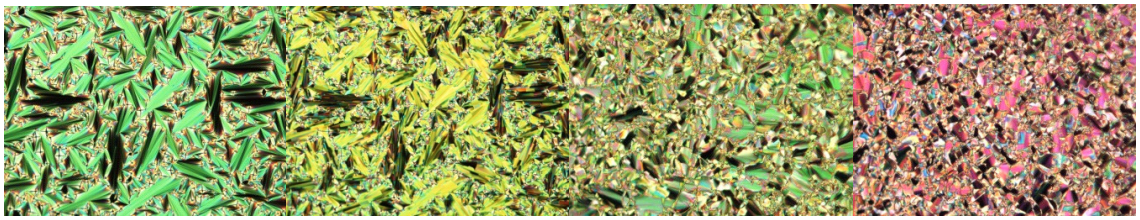

(a) **(b)** **(c)** **(d)**

Figure 4. Pictures taken at the polarizing optical microscope showing the optical textures of complex **2c** at 55°C (a) and at 47°C (b), complex **3b** at 95°C (c) and complex **3c** at 62°C (d).

Next step was to use the branched alkoxy-substituted BTU derivatives with the aim of reducing the transition temperatures and to avoid a possible thermal decomposition of these products. Moreover, we were interested to find if the smectic C phase could be stabilized over a longer range of temperatures in view of later preparation of Pd(II) and Pt(II) complexes displaying chiral smectic C phase. Indeed, the new complexes **2a-b** display only a monotropic SmC phase on cooling from liquid state with very sharp transitions to mesophase. Both the melting points and transition temperatures were reduced. For instance, the melting point of **2a** is lowered by 33°C compare to its analogue **1a**, while for **2b** the melting point dropped by 41°C compared to **1b**. In addition, the transition to SmC phase for **2a,b** occurred at temperatures that are lowered by almost 40°C than the corresponding **1a,b**. **2c** was found to show both SmA and SmC phases at considerable lower temperatures, around 40°C in respect to **1c**. These two phases were found to be stable both on heating and cooling after the initial melting process and, very important, the SmC phase was stable up to room temperature when transformed into a

glassy state. The following two heating-cooling cycles showed that the two phases are perfectly reversible and no crystallization occurs on supercooling the sample. Encouraged by these results, we decided to prepare the Pt(II) analogues with branch BTU derivative in order to take advantage of the possible luminescence properties of such complexes. Indeed, the Pt analogues **3a, b** show perfectly the same liquid crystal properties with slightly higher transition temperatures. This is the result of replacing palladium with the heavier platinum metal responsible for the polarization enhancement. On the contrary, on cooling the complex **3c**, a slow, thermodynamically driven, crystallization process was seen around 56°C. Complex **4** exhibits a monotropic smectic A phase on cooling from the isotropic liquid stable up to room temperature, while crystallization occurs on reheating the sample and this was clearly seen on the second heating-cooling DSC cycle (see Figure S11 in ESI).

Table 4 Powder X-ray diffraction data for Pd(II) and Pt(II) complexes

Complex	T/°C	Phase	2θ/°	d spacing/ Å	Indexation
1a	80	Cr	2.50	35.3	(001)
			5.04	17.5	(002)
			7.62	11.6	(003)
			10.20	8.7	(004)
1b	80	SmC	3.76	23.5	(001)
			7.64	11.6	(002)
1c	70	SmC	3.92	22.5	(001)
			7.94	11.1	(002)
2a	80	SmC	3.28	27.3	(001)
			6.52	13.7	(002)
			9.82	9.1	(003)
2b	80	SmC	3.36	26.6	(001)
			6.78	13.2	(002)
			10.22	8.6	(003)
2c	50	SmC	3.12	28.7	(001)
			6.26	14.2	(002)
			9.44	9.4	(003)
3a	80	SmC	4.04	22.1	(001)
			8.16	11.0	(002)
3b	80	SmC	3.84	23.3	(001)
			7.76	11.5	(002)
3c	60	SmC	4.18	21.4	(001)
			8.46	10.6	(002)
4	25	SmA	3.74	23.9	(001)
			7.46	12.0	(002)

The direct transition from the Isotropic to Smectic phases (I–SmA, I–SmC, I–SmC*) is well characterized as a strongly first-order transition for chiral or non- chiral liquid crystals.

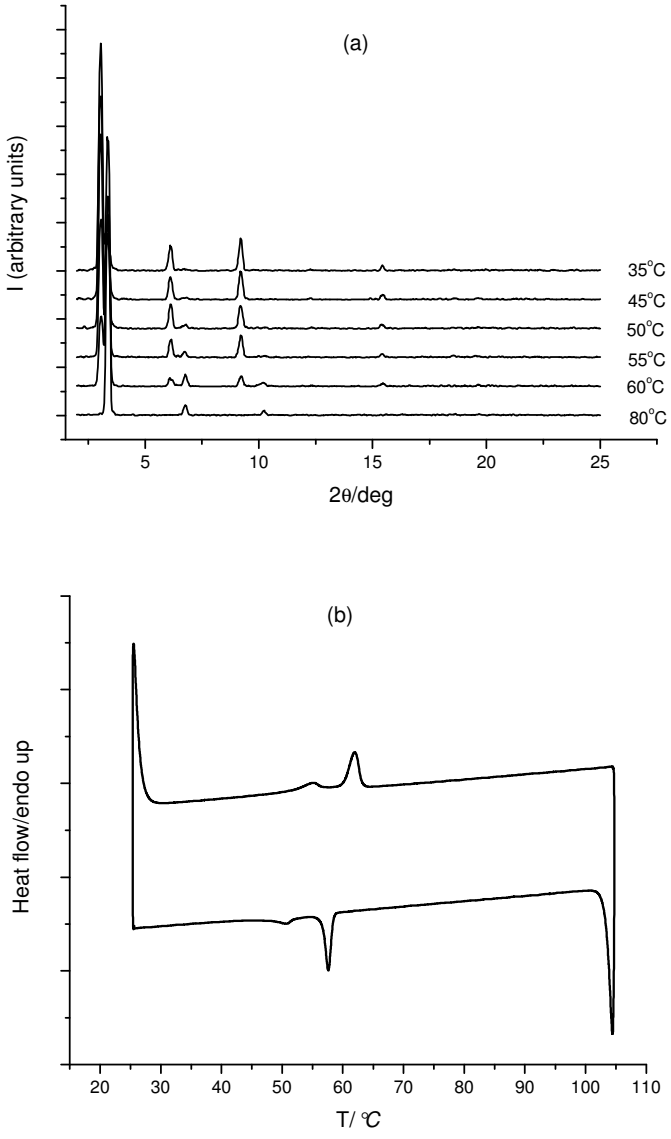

Figure 5. Powder X-ray diffractogram of complex **2b** recorded at various temperature on cooling from isotropic liquid (a) and DSC trace (second heating – cooling cycle) of complex **2c** (b).

All the phases assignment done by POM were confirmed by X-ray studies. Powder X-Ray diffraction studies were performed on cooling the samples from the isotropic liquid

to the mesophase. The X-ray patterns for all Pd(II) and Pt(II) compounds show two or three signals in the low angle region equally spaced in the 1:2:3 ratio assigned to d_{001}, d_{002} and d_{003} that is typical for a lamellar structure. This observation indicates a layer structure, whereby the interlayer spacing is comparable to the molecule length obtained by molecular modeling in all-trans conformation.

Along with these reflections, a broad peak around 4.6 Å corresponding to the molten state of the chains was also observed in the X-ray pattern of all complexes with the exception of complex **1a**. As this complex crystallizes rapidly on cooling, we were able to record only the X-ray diffractogram of the crystalline state (see Table 4). In addition, several samples were subject to variable temperature X-ray analysis to clearly establish the nature of the smectic phase. For instance, **3a** showed a pronounced decrease of the layer thickness given by the measured d-spacing on cooling the sample from 100 to 70°C, typical for the tilted SmC phase (Table 1 ESI). Generally, on cooling further, the X-ray powder pattern shows typical signals assigned to both liquid crystalline and crystalline phases, and one example, for complex **2b**, is shown in Figure 5(a).

The d-spacing for Pt(II) complexes, all show a significant lower values when compare to Pd(II) analogues probably due to a higher tilt angles combined with some more pronounced interdigitation of alkyl chains.

Photophysical properties

The photophysical properties of Pt(II) complexes in solid state, solution in dichloromethane and PMMA films have been investigated and the results are summarized in Table 5. All six Pd(II) complexes show no emission at room temperature and this is not surprising as it is known that emissive Pd(II) complexes at room temperature are much rarer when compare to Pt(II) complexes.[18]

The UV-VIS absorption spectra of Pt(II) complexes recorded in CH_2Cl_2 feature two highly intense absorption bands at around λ_{max} 290 ($\varepsilon > 16.9 \times 10^3$ mol^{-1} dm^3 cm^{-1}) and 319-335 nm range ($\varepsilon > 11.5 \times 10^3$ mol^{-1} dm^3 cm^{-1}) that are assigned to ^{1}LC($\pi\pi^*$) ligand centered transitions of the cyclometalated and BTU ligands, based on similarities with the absorptions of the free ligands. Sometimes, these are seen like shoulders probably due to broadening resulted from the superposition of π–π^* transitions of the two different

coordinated ligands. In addition, a moderately intense band that is absent for the ligands is observed at λ_{max} 390 nm ($\varepsilon > 5.2 \times 10^3$ mol^{-1} dm^3 cm^{-1}), with a shoulder in the 443 - 469 nm range ($\varepsilon > 1.2 \times 10^3$ mol^{-1} dm^3 cm^{-1}). These less intense low-energy absorptions located at $\lambda > 350$ nm could be assigned to a mixture of spin-allowed metal-to-ligand charge transfer (^{1}MLCT) and ligand-centered (^{1}LC) transitions, and this assignment is consistent with previous results based on related cyclometalated Pt(II) compounds.[4d] Solid-state and PMMA film emission spectra recorded at room temperature for complexes **3a-c** are shown in Figure 6.

The emission spectra of all four Pt(II) complexes show two maxima at λ_{max} around 480-530 and 615 - 633 nm respectively, when the samples were irradiated in the 380-420 nm region. This red emission has also been visually detected at the optical microscope when the samples were irradiated in the 380-420 nm region (Figure S15 ESI). It was found that the emission bands slightly red-shift with increasing number of alkoxy chains in the molecules. The luminescence spectra recorded in solid state show two emission maxima situated around λ_{max}=610 nm and λ_{max}=655 nm, except complex **3b** which shows a broad emission centered at λ_{max} = 629 nm slightly red-shifted compare to spectra recorded in dichloromethane solution at room temperature. The measured quantum yields in dichloromethane solution are rather low, but comparable with other Pt(II) complexes with Schiff bases ligands.[19] On the other hand, the Pt(II) complexes display less intense broad emission in PMMA films (10% wt.) around λ_{max} =650 nm for complexes **3a-c** and λ_{max} =627 nm for complex **4**, when recorded at room-temperature.

Table 5. Photophysical properties of Pt(II) complexes

Compound	Absorption, λ_{max}/nm (εx10^{-3}/M^{-1}·cm^{-1})	Emission, λ_{em}/nm solution (λ_{exc}/nm; Φ/%)[a]	solid	PMMA film
3a	294(sh, 16.9), 319(17.3), 387 (9.7), 443(sh, 2.10)	615(387/0.7)	610, 652	642
3b	290(114.3), 335 (sh, 33.5), 387(12.9), 447(sh, 2.4),	615(387/0.6)	629	655
3c	287(65.0), 330 (sh, 17.2), 394(5.2), 467(sh,1.2)	632(394/0.6)	615, 655	648
4	279(sh, 22.3), 325 (sh, 11.5), 392(6.7), 469(sh, 1.3)	633(392/0.8)	603 (sh), 640	627

[a]Quantum yields were determined with respect to $[Ru(bpy)_3]^{2+}$ in water

To get further information regarding the relationship between the emission properties and morphology, we investigated the luminescence spectra of complex **4** in crystalline state

and in liquid crystalline phase after heating above the isotropic temperature and cooling down to room temperature, taking advantage of mesophase stability at room temperature (Figure 7). We didn't notice any shift in the emission position on going from crystalline state to liquid crystal phase and to isotropic, except a normal decrease of the emission intensity with increasing the sample temperature. Thus, it is difficult to make any assumption regarding a possible aggregation or excimer contribution emission due to self-assembled structure of the liquid crystalline phase as reported in other liquid-crystalline Pt(II) complexes.[4j,k]

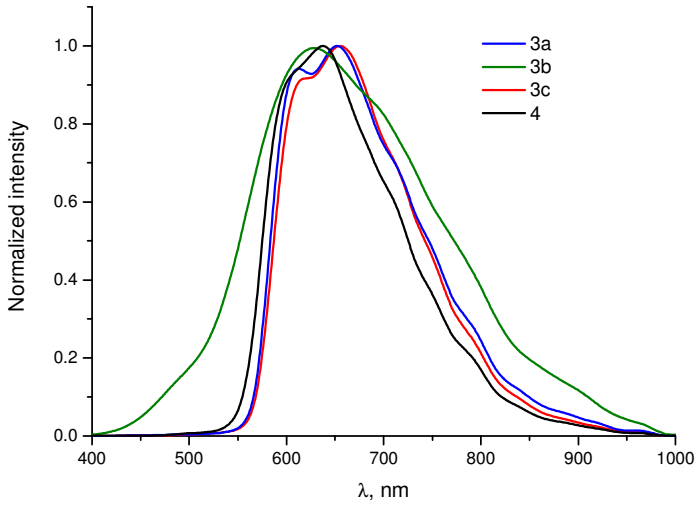

(a)

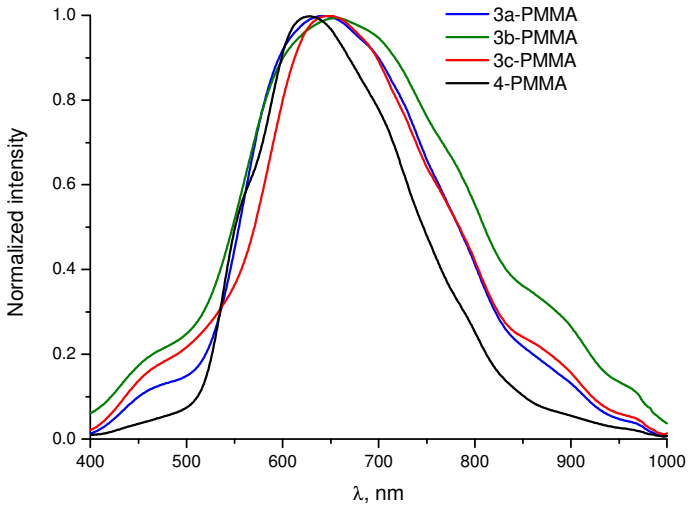

(b)

Figure 6. Solid state (a) and PMMA films (b) emission spectra for Pt(II) complexes

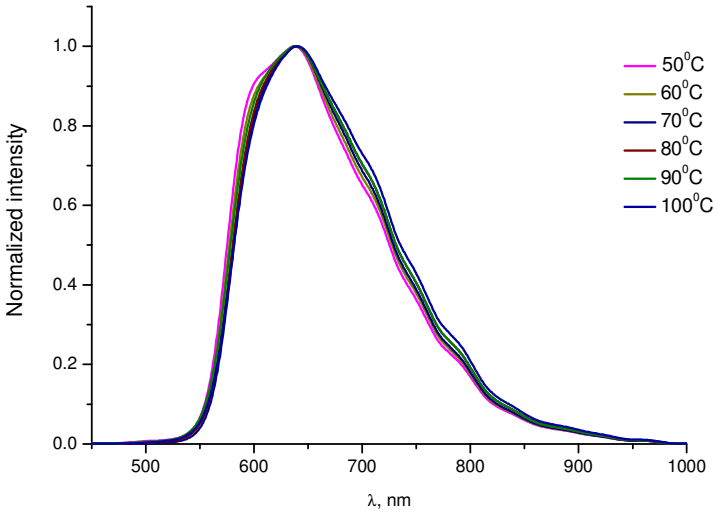

Figure 7. The normalized emission spectra of complex 4 at various temperatures

Experimental:

All the chemicals were used as supplied. C, H, N analyses were carried out with a Perkin Elmer instrument. IR spectra were recorded on a Bruker spectrophotometer using ATR technique. UV-VIS absorption spectra were recorded by using a Jasco V-660

spectrophotometer. ^{1}H and ^{13}C NMR spectra were recorded on a Varian Gemini 300 BB spectrometer operating at 300 MHz, using $CDCl_3$ as solvent. ^{1}H chemical shifts were referenced to the solvent peak position, δ 7.26 ppm. The phase assignments and corresponding transition temperatures for the palladium(II) complexes were determined by polarizing optical light microscopy (POM) using a Nikon 50iPol microscope equipped with a Linkam THMS600 hot stage and TMS94 control processor. Temperatures and enthalpies of transition were investigated using differential scanning calorimetry (DSC) with a Diamond DSC Perkin Elmer. The materials were studied at scanning rates of 5 and 10°C/min after being encapsulated in aluminium pans. Two or more heating/cooling cycles were performed on each sample. Mesophases were assigned by their optical texture and powder X-ray diffraction studies.

The powder X-ray diffraction measurements were made on a D8 Advance diffractometer (Bruker AXS GmbH, Germany), in parallel beam setting, with monochromatized Cu–$K_{\alpha 1}$ radiation (λ=1.5406 Å), scintillation detector, and horizontal sample stage. The measurements were performed in symmetric (θ-θ) geometry in the 2θ range from 1.5^{o} to 10^{o} or 25^{o} in steps of 0.02^{o}, with measuring times per step in the 5-40 s range. The temperature control of the samples during measurements was achieved by adapting a home-made heating stage to the sample stage of the diffractometer. X-ray single-crystal data for **4** were collected with a Bruker-AXS APEXII diffractometer. The structure was solved by direct methods using the *SIR97* program,[20] and then refined with full-matrix least-square methods based on F^2 (*SHELXL-97*)[21] with the aid of the *WINGX*[22] program. All non-hydrogen atoms were refined with anisotropic atomic displacement parameters. H atoms were finally included in their calculated positions. Luminescence spectra were recorded on a Fluorolog-3™ fluorescence spectrometer (FL3-22, Horiba Jobin Yvon) in solid state and employing a Jasco FP-6300 spectrofluorimeter (operating parameters: band width – 5 nm; data pitch – 0.5 nm; scanning speed – 100 nm/min; spectrum accumulation – 3; path length – 10 mm by using Quartz SUPRASIL cells) in dichloromethane solution. Variable temperature emission spectra were recorded with an OceanOptics USB4000 spectrometer attached to the microscope and using a Nikon Intensilight excitation source. Thermogravimetric analysis was performed on a TA Q50

instrument. The heating rate employed was 10°C min^{-1} from room temperature (approximately 25°C).

Synthesis of Pd(II) complexes 1a-c, 2a-c

Corresponding solid *N*-benzoylthiourea compound (0.30 mmol) was added to a suspension of dinuclear μ-acetato-bridged palladium complexes (0.10 mmol) and K_2CO_3 in dichloromethane (15 cm^3) and the mixture stirred at room temperature for 24 hours. Evaporation of the solvent gave a yellow solids, which were purified by chromatography on silica using dichloromethane as eluant to yield the final products. They were further crystallized from a mixture of dichloromethane/ethanol (1/1) at –25ºC.

Synthesis of Pt(II) complexes 3a-c, 4

To a methanolic solution of $[Pt(\mu\text{-}Cl)(\eta^3\text{-}C_4H_7)]_2$ (0.057g, 0.1 mmol in 20ml) corresponding solid imine ligand (0.25 mmol) was added and the suspension was stirred at room temperature for 48h. The resulting orange-brown solid was filtered off, washed several times with cold methanol and dried. This product was reacted further with an excess amount of corresponding BTU derivative (0.25 mmol) in dichloromethane to give orange crystalline solids which were purified on silica by using dichloromethane as eluant. The final products were obtained by crystallization from a mixture of acetone/methanol (1/1) at -25°C.

1a Yield 55%. Calc. for $C_{51}H_{77}N_3O_5PdS$: %C: 64.43; %H 8.16; %N 4.42. Found: %C 64.05; %H 8.37; %N 4.53.

^{1}H-NMR ($CDCl_3$, 300 MHz): 8.13 (s, 1H), 7.90 (s, br, 1H), 7.65 (d, br, 2H), 7.49-7.33 (m, 5H), 6.98 (d, J=8.5Hz, 2H), 6.90 (d, J=8.3Hz, 2H), 6.69 (d, J=8.8Hz, 2H), 6.60 (dd, ^{3}J=8.0Hz, ^{4}J=2.1Hz, 1H), 4.06-3.92 (m, 8H), 1.90-1.82 (m, 8H), 1.55-1.25 (m, 32H), 0.95-0.90 (m, 12H).

IR (ATR, cm^{-1}): 2955, 2929, 2856, 1605, 1583, 1541, 1507, 1473, 1422, 1311, 1296, 1247, 1167, 1109, 1034, 913, 834, 793, 768, 669, 576, 518.

1b Yield 67%. Calc. for $C_{59}H_{85}N_3O_5PdS$: %C: 67.18; %H 8.12; %N 3.98. Found: %C 67.25; %H 7.86; %N 4.18.

^{1}H-NMR ($CDCl_3$, 300 MHz): 8.11 (s, 1H), 7.92 (s, br, 1H), 7.65 (d, br, 2H), 7.49-7.33 (m, 5H), 6.98 (d, J=8.5Hz, 2H), 6.90 (d, J=8.3Hz, 2H), 6.69 (d, J=8.8Hz, 2H), 6.61 (dd,

^{3}J=8.0Hz, ^{4}J=2.4Hz, 1H), 4.06-3.92 (m, 8H), 1.90-1.82 (m, 8H), 1.55-1.25 (m, 40H), 0.95-0.90 (m, 12H).

IR (ATR, cm^{-1}): 2957, 2922, 2853, 1600, 1585, 1540, 1504, 1472, 1416, 1313, 1236, 1209, 1165, 1108, 1031, 964, 910, 836, 789, 765, 721, 660, 623, 567, 519.

1c Yield 72%. Calc. for $C_{73}H_{113}N_3O_6PdS$: %C: 69.19; %H 8.99; %N 3.32. Found: %C 68.85; %H 8.80; %N 3.18.

^{1}H-NMR ($CDCl_3$, 300 MHz): 8.05 (s, 1H), 7.66 (br, 2H), 7.42 (d, J=8.9Hz,2H), 7.37 (d, J=8.8Hz, 2H), 6.99 (s, 1H), 6.97 (d, J=8.9Hz, 2H), 6.91-6.85 (m, 3H), 6.68 (d, J=8.9Hz, 2H), 4.10-3.85 (m, 10H), 1.85-1.20 (m, 69H), 0.92-0.82 (m, 18H).

^{13}C NMR: 171.3, 162.4, 158.5, 151.4, 149.9, 146.3, 141.7, 139.0, 132.3, 130.0, 129.9, 126.0, 124.5, 124.4, 117.2, 115.7, 115.1, 114.8, 114.6, 113.6, 70.4, 69.0, 68.7, 68.5, 68.3, 32.2, 32.1, 29.9, 29.7, 29.6, 29.5, 29.4, 29.3, 26.4, 22.9, 14.3.

IR (ATR, cm^{-1}): 2921, 2853, 1601, 1537, 1504, 1464, 1389, 1318, 1242, 1212, 1156, 1104, 1070, 1024, 992, 908, 852, 829, 772, 720, 668, 630, 570, 517.

2a Yield 71%. Calc. for $C_{51}H_{77}N_3O_5PdS$: %C: 64.43; %H 8.16; %N 4.42. Found: %C 64.15; %H 8.43; %N 4.25.

^{1}H-NMR ($CDCl_3$, 300 MHz): 8.12 (s, 1H), 7.92 (s, br, 1H), 7.65 (d, br, 2H), 7.46-7.33 (m, 5H), 6.98 (d, J=8.9Hz, 2H), 6.89 (d, br, 2H), 6.70 (d, J=8.9Hz, 2H), 6.60 (dd, ^{3}J=8.0Hz, ^{4}J=2.1Hz, 1H), 4.06-3.95 (m, 6H), 3.84 (d, J=5.5Hz, 2H), 1.90-1.25 (m, 37H), 0.97-0.85 (m, 15H).

^{13}C-NMR ($CDCl_3$, 75MHz): 171.2, 160.4, 140.2, 132.4, 130.6, 124.6, 119.1, 114.9, 114.7, 113.7, 111.1, 70.7, 68.6, 68.2, 39.6, 32.0, 31.8, 30.7, 29.6, 29.5, 29.3, 26.3, 26.0, 25.9, 24.1, 23.2, 22.9, 22.8, 18.7, 14.3.

IR (ATR, cm^{-1}): 2956, 2925, 2858, 1603, 1581, 1537, 1503, 1459, 1405, 1296, 1239, 1198, 1163, 1103, 1029, 911, 830, 768, 719, 719, 698, 672, 561, 516.

2b Yield 73%. Calc. for $C_{59}H_{85}N_3O_5PdS$: %C: 67.18; %H 8.12; %N 3.98. Found: %C 67.05; %H 8.25; %N 4.13.

^{1}H-NMR ($CDCl_3$, 300 MHz): 8.10 (s, 1H), 7.93 (s, br, 1H), 7.63 (d, br, 2H), 7.44-7.31 (m, 5H), 6.96 (d, J=8.8Hz, 2H), 6.87 (d, br, 2H), 6.69 (d, J=8.9Hz, 2H), 6.59 (dd, ^{3}J=8.0Hz, ^{4}J=2.0Hz, 1H), 4.06-3.95 (m, 6H), 3.83 (d, J=5.8Hz, 2H), 1.90-1.25 (m, 45H), 0.95-0.85 (m, 15H).

^{13}C-NMR ($CDCl_3$, 75MHz): 171.2, 162.6, 141.7, 140.2, 132.3, 130.5, 124.5, 119.1, 114.9, 114.7, 113.6, 111.0, 68.8, 68.3, 39.6, 32.0, 29.6, 29.5, 29.4, 29.3, 26.3, 26.2, 24.1, 23.2, 22.9, 22.8, 14.3.

IR (ATR, cm^{-1}): 2957, 2923, 2855, 1603, 1581, 1538, 1504, 1459, 1406, 1297, 1240, 1199, 1105, 1031, 966, 911, 831, 768, 719, 698, 673, 562, 517.

2c Yield 81%. Calc. for $C_{73}H_{113}N_3O_6PdS$: %C: 69.19; %H 8.99; %N 3.32. Found: %C 68.92; %H 8.75; %N 3.09.

^{1}H-NMR ($CDCl_3$, 300 MHz): 8.07 (s, 1H), 7.64 (br, 2H), 7.45 (d, J=8.9Hz,2H), 7.38 (d, J=8.8Hz, 2H), 7.0 (s, 1H), 6.97 (d, J=8.9Hz, 2H), 6.90-6.85 (m, 3H), 6.70 (d, J=8.9Hz, 2H), 4.08-3.92 (m, 8H), 3.83 (d, J=6.0Hz, 2H), 1.90-1.20 (m, 69H), 0.95-0.85 (m, 18H).

IR (ATR, cm^{-1}): 2953, 2922, 2853, 1627, 1603, 1504, 1466, 1402, 1302, 1241, 1219, 1166, 1098, 1069, 975, 952, 911, 855, 828, 789, 735, 661, 633, 604, 558, 527.

3a Yield 31%. Calc. for $C_{51}H_{77}N_3O_5PtS$: %C: 58.94; %H 7.47; %N 4.04. Found: %C 58.63; %H 7.85; %N 3.86.

^{1}H-NMR ($CDCl_3$, 300MHz): 8.36 (s, $^{3}J_{PtH}$=112Hz, 1H), 7.91 (s, br, 1H), 7.51 (d, br, 2H), 7.45-7.34 (m, 5H), 6.98 (d, J=8.7Hz, 2H), 6.90 (d, J=8.8Hz, 2H), 6.67 (d, J=8.8Hz, 2H), 6.58 (dd, ^{3}J=8.2Hz, ^{4}J=2.2Hz, 1H), 4.06-3.95 (m, 6H), 3.82 (d, J=5.8Hz, 2H), 1.85-1.65 (m, 7H), 1.58-1.25 (m, 30H), 0.95 (m, 15H).

^{13}C-NMR ($CDCl_3$, 75MHz): 162.5, 158.5, 141.1, 132.7, 132.1, 130.9, 130.1, 125.0, 114.8, 114.7, 113.7, 70.6, 68.7, 68.5, 68.0, 39.5, 32.0, 31.8, 30.7, 30.6, 29.6, 29.5, 29.4, 29.2, 26.3, 25.9, 25.8, 24.0, 23.2, 22.8, 14.2.

IR (ATR, cm^{-1}): 2955, 2924, 2858, 1603, 1584, 1532, 1502, 1457, 1407, 1298, 1241, 1198, 1163, 1103, 1027, 911, 830, 767, 698, 673, 515.

3b Yield 42%. Calc. for $C_{59}H_{85}N_3O_5PtS$: %C: 61.97; %H 7.49; %N 3.67. Found: %C 61.53; %H 7.64; %N 3.51.

^{1}H-NMR ($CDCl_3$, 300 MHz): 8.37 (s, $^{3}J_{PtH}$=118Hz, 1H), 7.90 (s, br, 1H), 7.54 (d, br, 2H), 7.44-7.34 (m, 5H), 6.98 (d, J=8.8Hz, 2H), 6.90 (d, J=8.8Hz, 2H), 6.67 (d, J=8.8Hz, 2H), 6.58 (dd, ^{3}J=8.2Hz, ^{4}J=2.2Hz, 1H), 4.06-3.95 (m, 6H), 3.83 (d, J=5.8Hz, 2H), 1.85-1.65 (m, 7H), 1.58-1.25 (m, 38H), 0.95 (m, 15H).

^{13}C-NMR ($CDCl_3$, 75MHz): 162.5, 158.5, 141.2, 132.7, 132.1, 130.9, 130.1, 125.1, 114.8, 114.7, 113.7, 70.6, 68.7, 68.5, 39.5, 32.0, 31.8, 30.7, 30.6, 29.6, 29.5, 29.4, 29.2, 26.3, 25.9, 25.8, 25.7, 24.0, 23.2, 22.8, 14.2.

IR (ATR, cm^{-1}): 2956, 2922, 2855, 1602, 1583, 1533, 1502, 1455, 1406, 1299, 1197, 1164, 1104, 1042, 1027, 911, 831, 768, 721, 699, 631, 516.

3c Yield 37%. Calc. for $C_{73}H_{113}N_3O_6PtS$: %C: 64.67; %H 8.40; %N 3.10. Found: %C 64.35; %H 8.17; %N 2.88.

^{1}H-NMR ($CDCl_3$, 300 MHz): 8.07 (s, 1H), 7.93 (s, br, 1H), 7.64 (br, 2H), 7.45 (d, J=8.9Hz,2H), 7.38 (d, J=8.8Hz, 2H), 7.0 (s, 1H), 6.97 (d, J=8.9Hz, 2H), 6.90-6.85 (m, 3H), 6.70 (d, J=8.9Hz, 2H), 4.08-3.92 (m, 8H), 3.83 (d, J=6.0Hz, 2H), 1.90-1.20 (m, 69H), 0.95-0.85 (m, 18H).

^{13}C-NMR ($CDCl_3$, 75MHz): 158.2, 157.6, 152.0, 149.5, 145.2, 129.8, 123.8, 122.0, 115.0, 122.0, 115.0, 112.6, 111.3, 69.2, 68.4, 31.9, 29.6, 29.5, 29.4, 29.3, 29.2, 26.1, 26.0, 22.7, 14.1.

IR (ATR, cm^{-1}): 2957, 2920, 2852, 1622, 1602, 1576, 1506, 1466, 1435, 1403, 1298, 1241, 1222, 1166, 1135, 1070, 854, 828, 771, 737, 722, 603, 558, 526.

4 Yield 35%. Calc. for $C_{49}H_{64}N_3O_4PtS$: %C: 58.55; %H 6.42; %N 4.18. Found: %C 58.17; %H 6.15; %N 3.96.

^{1}H NMR ($CDCl_3$, 300 MHz): 8.08 (1H, s), 7.70 (2H, m), 7.56– 7.48 (2H, m), 7.40–7.36 (3H, m), 7.23 (2H, t br), 7.07 (2H, t, AA'MXX', J = 8.6 Hz), 7.00 (1H, s), 6.97 (2H, d, AA'XX', J = 8.8 Hz), 6.85 (1H, s br), 4.12 (2H, m), 4.02 (2H, t, J = 6.6 Hz), 3.94 (2H, t, J = 6.7 Hz), 1.90–1.25 (30H, m), 0.89 (15H, m).

IR (ATR, cm^{-1}): 2958, 2920, 2853, 1622, 1602, 1586, 1536, 1427, 1299, 1197, 1164, 1104, 1042, 1028, 911, 831, 775, 721, 699, 635, 516.

Conclusions

A novel series of Pd(II) and Pt(II) complexes based on cyclometalated imine ligands and N-benzoylthiourea (BTU) derivatives as auxiliary ligands has been prepared and their liquid crystalline properties as well as photophysical properties have been investigated. We were able to show that comparable emission properties with other systems reported in the literature based on Schiff bases can be achieved in simpler Pt(II) systems making

them interesting candidates for possible applications in electro-optical devices. Moreover, the liquid crystalline properties could be improved by replacing the alkoxy terminal groups with branched alkyl chains. In this way, the transition temperatures could be lowered and, thus, preventing the partial decomposition observed for the Pd(II) complexes with *n*-alkyl chains in terminal positions. Additionally, the stabilization of the smectic C phase over a relatively large temperature range found in the case of branched alkoxy derivatives could be used in the future to prepare liquid crystalline materials displaying chiral smectic C phase (SmC*).

Appendix A. Supplementary data

CCDC 963300 contains the supplementary crystallographic data for complex **4**. These data can be obtained free of charge via http://www.ccdc.cam.ac.uk/conts/retrieving.html, or from the Cambridge Crystallographic Data Centre, 12 Union Road, Cambridge CB2 1EZ, UK; fax: (+44) 1223-336-033; or e-mail: deposit@ccdc.cam.ac.uk. Electronic Supplementary Information (ESI) available: DSC and TG curves, polarizing microscopy pictures and powder X-ray diffraction data at various temperatures.

Acknowledgments

This work was supported by a grant of the Romanian Authority for Scientific Research, CNCS-UEFISCDI, project number PN-II-ID-PCE-2011-3-0384.

References:

1 S. Laschat, A. Baro, N. Steinke, F. Giesselmann, C. Hagele, G. Scalia, R. Judele, E. Kapatsina, S. Sauer, A. Schreivogel, M. Tosoni, *Angew. Chem. Int. Ed.*, 46 (2007) 4832.

2 B. Donnio, D. Guillon, R. Deschenaux, D.W. Bruce in Comprehensive Coordination Chemistry II, J.A. McCleverty, T.J. Meyer (Eds). Vol. 7, Chap. 7.9, pp. 357–627, Elsevier, Oxford (2003); B. Donnio, D. Guillon, R. Deschenaux and D. W. Bruce, in Comprehensive Organometallic Chemistry III, vol. 12, ed. R. H. Crabtree, and D. M. P. Mingos Elsevier, Oxford, UK, ch. 12.05, pp.195 – 293 (2006).

3 K. Binnemans, *J. Mater. Chem.*, 19 (2009) 448.

4 V. N. Kozhevnikov, B. Donnio, D. W. Bruce, *Angew. Chem. Int. Ed.*, 47 (2008) 6286; A. Santoro, A.C. Whitwood, J.A. Gareth Williams, V.N. Kozhevnikov, D.W. Bruce, *Chem. Mater.*, 21 (2009) 3871; C. Damm, G. Israel, T. Hegmann, C. Tschierske, *J. Mater. Chem.*, 16 (2006) 1808; A. S. Mocanu M. Ilis, F. Dumitrascu, M. Ilie, V. Circu, *Inorg. Chim. Acta*, 363 (2010) 729; V. Cîrcu, P.N. Horton, M.B. Hursthouse, D.W. Bruce, *Liq. Cryst.*, 34 (2007) 1463; J. Buey, L. Diez, P. Espinet, H.-S. Kitzerow, J.A. Miguel, *Chem. Mater.*, 8 (1996) 2375; L. Diez, P. Espinet, J.A. Miguel and M.B. Ros, *J. Mater. Chem.,* 12 (2002) 3694; Y. Wang, Y. Liu, J. Luo, H. Qi, X. Li, M. Nin, M. Liu, D. Shi, W. Zhu and Y. Cao, *Dalton Trans*., 40 (2011) 5046; Y. Wang, Q. Chen, Y. Li, Y. Liu, H. Tan, J. Yu, M. Zhu, H. Wu, W. Zhu, Y. Cao, *J. Phys.Chem. C*, 116 (2012) 5908; K. Venkatesan, P.H.J. Kouwer, S. Yagi, P. Muller, T. M. Swager, *J. Mater. Chem*., 18 (2008) 400; B. Bilgin-Eran, H. Ocak, C. Tschierske, U. Baumeister, *Liq. Cryst.*, 39 (2012) 467; K. Praefcke, B. Bilgin, J. Pickardt, M. Borowski, *Chem. Ber.*, 127 (1994) 1543.

5 V. Cîrcu, D. Manaila-Maximean, C. Rosu, M. Ilis, Y. Molard, F. Dumitrascu, *Liq. Cryst*., 36 (2009)123.

6 L. Beyer, E. Hoyer, J. Liebscher, H. Hartmann, *Z. Chem.*, 21 (1981) 81; P. Muhl, K. Gloe, F. Dietze, E. Hoyer, L. Beyer, *Z. Chem.*, 26 (1986) 81; K.R. Koch, *Coord. Chem. Rev.*, 216 - 217 (2001) 473.

7 V. Cîrcu, M. Ilis, F. Dumitrascu, *J. Optoelectron. Adv. Mater.*, 10 (2008) 3454; A.C. Tenchiu, M. Ilis, F. Dumitrascu, A.C. Whitwood, V. Cîrcu, *Polyhedron*, 27 (2008) 3537.

8 T. Seshadri, H.-J. Haupt, *J. Mater. Chem.*, 8 (1998) 1345; A. Deleanu, M. Ilis, T. Rosu, V. Cîrcu, *Rev. Chim.(Bucharest)*, 57 (2006) 1216; T. Seshadri, H.-J. Haupt, U. Flörke, G. Henkel, *Liq. Cryst.*, 34 (2007) 33.

9 P.J. Collings, M. Hird, *Introduction to Liquid Crystals Chemistry and Physics*, Taylor&Francis, London and New York, (2004) M. Ghedini, D. Pucci, E. Cesarotti, O. Francescangeli, R. Bartolino, *Liq. Cryst.* 15 (1993) 331; S. Hayami, R. Moriyama, A. Shuto, Y. Maeda, K. Ohta, K. Inoue, *Inorg. Chem.*, 46 (2007) 7692; F. Camerel, R.

Ziessel, B. Donnio, C. Bourgogne, D. Guillon, M. Schmutz, C. Iacovita, J.-P. Bucher, Angew. Chem. Int. Ed., 46 (2007) 2659.

10 D.J. Mabbot, B.E. Mann, P.M. Maitlis, *J. Chem. Soc., Dalton Trans.*, (1977) 294.

11 P.S. Pregosin, F. Wombacher, A. Albinati, F. Lianza. *J. Organomet. Chem.*, 418 (1991) 249.

12 A. Capape, M. Crespo, J. Granell, M. Font – Bardia, X. Solan, *Dalton Trans.*, (2007) 2030; R. Martin, M. Crespo, M. Font-Bardia, T. Calvet, *Organometallics*, 28 (2009) 589; M. Crespo, M. Font-Bardia, X. Solans, *J. Organomet. Chem.*, 691 (2006) 444; K. Praefcke, B. Bilgin, J. Pickardt, M. Borowski, *Chem. Ber.*, 127 (1994) 1543.

13 C. Sacht, M. S. Datt, S. Otto, A. Roodt, *J.Chem. Soc., Dalton Trans.*, (2000) 727.

14 A. Irving, K. R. Koch, M. Matoetoe, *Inorg. Chim. Acta*, 206 (1993) 193.

15 V. Cîrcu, M. Ilie, M. Ilis, F. Dumitrascu, I. Neagoe, S. Pasculescu, *Polyhedron*, 28 (2009) 3739.

16 A. Bondi, *J. Phys. Chem.*, 68 (1964) 441.

17 I. Dierking, Textures of Liquid Crystals, Wiley-VCH Verlag, Weinham, (2003).

18 D. Patra, P. Pattanayak, J.L. Pratihar, S. Chattopadhyay, *Polyhedron* 51 (2013) 46; M. Dolores Santana, R. Garcia-Bueno, G. Garcia, G. Sanchez, J. Garcia, J. Perez, L. Garcia, J. L. Serrano, *Inorg. Chim. Acta* 378 (2011) 49; M. Dolores Santana, R. Garcia-Bueno, G. Garcia, G. Sanchez, J. Garcia, A. R. Kapdi, M. Naik, S. Pednekar, J. Perez, L. Garcia, E. Perez, J. L. Serrano, *Dalton Trans.* 41 (2012) 3832; M. Dolores Santana, R. Garcia Bueno, G. Garcia, G. Sanchez, J. Garcia, J. Perez, L. Garcia, J. L. Serrano, *Dalton Trans.* 40 (2011) 3537; D.-Y. Ma, L.-X. Zhang, X.-Y. Rao, T. -L. Wu, D.-H. Li, X.-Q. Xie, *J. Coord. Chem.* 66 (2013) 1486 ; M. Micutz, M. Ilis, T. Staicu, F. Dumitrascu, I. Pasuk, Y. Molard, T. Roisnel, V. Cîrcu, *Dalton Trans.* (2014) doi :10.1039/c3dt52137k.

19 Yu Scaffidi-Domianello, A. A. Nazarov, M. Haukka, M. Galanski, B.K. Keppler, J. Schneider, P. Du, R. Eisenberg, V. Yu Kukushkin, *Inorg. Chem.* **2007**, *46*, 4469 – 4482; S. U. Pandya, K. C. Moss, M. R. Bryce, A. S. Botsanov, M. A. Fox, V. Jankus, H. A. Al Attar, A. P. Monkman, *Eur. J. Inorg. Chem.*, **2010**, 1963 – 1972.

20 A. Altomare, M. C. Burla, M. Camalli, G. Cascarano, C. Giacovazzo, A. Guagliardi, A. G. G. Moliterni, G. Polidori, R. Spagna, *J. Appl. Cryst.*, 32 (1999) 115.

21 SHELX97 - Programs for Crystal Structure Analysis (Release 97-2). G. M. Sheldrick, Institüt für Anorganische Chemie der Universität, Tammanstrasse 4, D-3400 Göttingen, Germany, (1998)

22 L. J. Farrugia, *J. Appl. Cryst.*, 32 (1999) 837.